Synthesis and biological evaluation of ^{18}F-FB-NGA as a hepatic asialoglycoprotein receptor PET imaging agent

GU Xiaobo[1] CAI Gangming[1] JIANG Mengjun[1,2]
ZHOU Yaoyuan[1] ZHANG Rongjun[1,*]

[1]*Key Laboratory of Nuclear Medicine, Ministry of Health, Jiangsu Key Laboratory of Molecular Nuclear Medicine, Jiangsu Institute of Nuclear Medicine, Wuxi 214063, China*

[2]*Department of Clinical Laboratory Science, the First Wuxi Affiliated Hospital of Nanjing Medical University, Wuxi Clinical Science Research Institute, Wuxi 214063, China*

Abstract Asialoglycoprotein receptor (ASGP-R) is a hepatic membrane receptor that uniquely exists on the surface of mammalian hepatocytes, and has been used as target of liver functional imaging agents for many years. We labeled the Galactosyl-neoglycoalbumin (NGA) with ^{18}F to get a PET molecular probe ^{18}F-FB-NGA and evaluated its ability as a liver functional PET imaging agent. The ^{18}F-FB-NGA was prepared with NGA by conjugation with *N*-succinimidyl-4-^{18}F-fluorobenzoate (^{18}F-SFB) and purified with PD-10 desalting column. The radiolabeling yield and radiochemical purity of ^{18}F-FB-NGA were determined by radio-HPLC. Starting with ^{18}F-F^{-}, the total time for ^{18}F-FB -NGA was about 120±10 min. The decay-corrected radiochemical yield is about 25–30%. The radiochemical purity of purified ^{18}F-FB-NGA was more than 98%. Labeled with 185–1850 MBq ^{18}F-SFB, the specific activity of ^{18}F -FB-NGA was estimated to be 7.83–78.3 TBq/mmol. Biodistribution of ^{18}F-FB-NGA in normal mice was investigated after injection through the tail vein. The results showed that the liver accumulated 39.47±3.42 and 12.12±6.11%ID/g at 10 and 30 min after injection, respectively. Dynamic MicroPET images in mice were acquired with and without block after injection of the radiotracer, respectively. High liver activity accumulation was observed at 5 min after injection in normal group. On the contrary, the liver accumulation was significantly lower after block, indicating the specific binding to ASGP-R. ^{18}F-FB-NGA is probably a potential PET liver imaging agent.

Key words Asialoglycoprotein receptor, 18F-FB-NGA, Biodistribution, PET Imaging

1 Introduction

Asialoglycoprotein is the glycoproteins with terminal galactose or *N*-acetylgalactosamine residues after removing the terminal sialic acid residues. Asialoglycoprotein receptor (ASGP-R), situated on the surface of hepatocyte membrane, can recognize and bind with asialoglycoprotein specifically. The number of ASGP-R on the hepatocytes of patients with liver disease is reduced and is thus considered as a specific indicator for evaluating liver function[1,2]. ASGP-R imaging agent can be used to evaluate the liver function and directly reflect the functional hepatocyte mass. Galactosyl-neoglycoalbumin (NGA) was synthesized as an analog ligand in 1976, and labeled with ^{99m}Tc for ASGP-R single photon emission computed tomography (SPECT) imaging. In 1992, a DTPA-conjugate of NGA (Diethylenetriaminepenta-acetic acid-Galactosyl human Serum Albumin, GSA) was introduced in Japan as a commercial product. ^{99m}Tc-GSA was the first commercially-available receptor-binding radiopharmaceutical[3–5]. We have prepared several derivates of glycoprotein for ASGP-R, such as ^{99m}Tc-NGA[6,7], galactosyl-human serum albumin-interferon-α2b (G-HSA-IFN)[8,9].

Supported by Jiangsu Province's Key Medical Talents Program (No. RC2007097), Natural Science Foundation of Jiangsu Province, China (No. BK2010154) and Science Foundation of Health Department of Jiangsu Province (No.H201226).

* Corresponding author. *E-mail address*: zhangrongjun@jsinm.org

Received date: 2012-10-15

Several ASGP receptor imaging agents have been reported for SPECT, but the images were not as good as positron emission tomography (PET) images. As a useful quantitative imaging tool, PET is a rapidly expanding clinical molecular imaging modality worldwide, and provides a much higher sensitivity (by approximately two to three orders of magnitude) and resolution than SPECT. As one of the most commonly used positron-emitting radionuclides for PET imaging, fluorine-18 (^{18}F) is widely used for labeling peptides and proteins PET probes, because of its positron emitting property, low energy (0.64 MeV) and favorable half-life (109.8 min). Peptides and proteins labeled by ^{18}F using prosthetic groups have achieved significant advances in recent years[10,11]. Among the available prosthetic groups, the acylation agent, succinimidyl-4-^{18}F-fluorobenzoate (^{18}F-SFB), is the most widely and frequently used[12–15].

Here, we report the synthesis of ^{18}F-FB-NGA by labeling NGA with the prosthetic group ^{18}F-SFB. The synthetic strategy was illustrated in Scheme 1. A semi-automated radio synthesis of ^{18}F-SFB was carried out on the ^{18}F-multifuntion synthesizer (Beijing PET Technology Co. Ltd., PRC) with a computer interface. The quality control was determined by radio high performance liquid chromatography[16]. Factors affecting the labeling yields of ^{18}F-FB-NGA, biological distribution and microPET imaging in mice were studied.

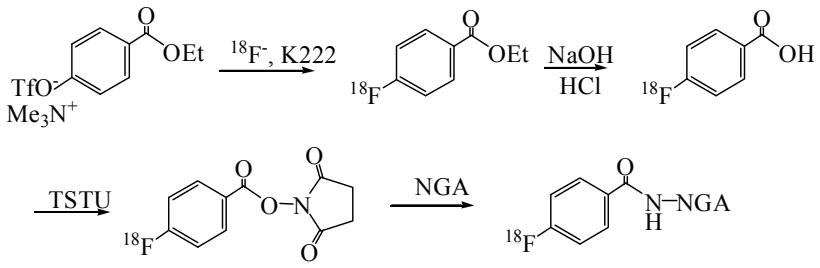

Scheme 1 Radiolabeling of ^{18}F-FB-NGA by active ester intermediate ^{18}F-SFB to coupling the ε-amide of lysine residue of NGA.

2 Materials and methods

2.1 Materials

All chemicals were obtained commercially and used without further purification. Methyl trifluoromethanesulfonate was purchased from Matrix Scientific. Ethyl 4-dimethylaminobenzoate was purchased from J & K Chemical LTD. Tetrapropylammonium hydroxide solution (1mol/L in water) was purchased from Aladdin Chemistry Co., Ltd. *N*, *N*, *N*′, *N*′-Tetramethyl-*O*-(*N*-succinimidyl) uranium tetrafluoroborate (TSTU) was purchased from Shanghai Medpep Co., Ltd. Ethyl 4-(trimethylammonium triflate) benzoate and unlabelled *N*-succinimidyl 4-fluorobenzoate (SFB) were synthesized according to the method of Haka *et al*.[17] and Johnstrom *et al*.[18], respectively. Galactosyl-neoglycoalbumin (NGA) was prepared by the procedures of Zhang *et al*.[6], with 25 galactose units attached to each molecule.

The analytical HPLC system included a binary HPLC pump (Waters 1525, USA), a UV detector (Waters 2487, USA) and a flow scintillation analyzer (Radiomatic 610TR, Perkin-Elmer, USA). Reversed-phase C-18 column (4.6× 250 mm, 5 μm particle size, Jiangsu Hanbon Science & Technology Co., Ltd) was eluted at a flow rate of 1mL/min as described in the experimental part. The absorbance was monitored at 254 nm. The TSKgel G2000SW$_{XL}$ column (7.8×300 mm) was purchased from TOSOH Corp., Japan. The Sep-Pak Light Waters Accell Plus QMA cartridge (Waters, USA) was activated with $NaHCO_3$ and water before use. Reversed-phase extraction Sep-Pak C18 Plus cartridges (Waters, USA) were activated with methanol and water before use. A PD-10 column (filled with Sephadex G25) was purchased from GE Healthcare. The ICR mice were provided by the Comparative Medicine Center of Yangzhou University.

2.2 Synthesis of 4-^{18}F-fluorobenzoic acid, ^{18}F-FBA

Automated synthesis of ^{18}F-labeling was carried out on an ^{18}F-multifuntion synthesizer (Beijing PET Technology Co. Ltd., PRC) with a computer interface.

The ^{18}F-F$^-$ was transferred in a pneumatic transport system from the cyclotron to the radiopharmaceutical laboratory. The ^{18}F-F$^-$ was separated from the ^{18}O–H_2O using an anion exchange cartridge (Sep-Pak Light Waters Accell Plus QMA cartridge). The synthesis program was started with the elution of ^{18}F-fluoride from the anion exchange cartridge into the reactor 1 using a solution of Kryprofix 222 (19.5 mg) and potassium carbonate (4.5 mg) in aqueous MeCN (1.5 mL, 90% MeCN) from vial 1 into the reaction vessel 1. The reaction vessel 1 was heated at 116°C and the solvent evaporated with a stream of nitrogen. The anhydrous MeCN (2 mL) was added from vial 2 and evaporated to dryness at 116°C for about 5 min. The solution of ethyl 4-(trimethylammoniumtriflate) benzoate 1 (10 mg) in anhydrous MeCN (1mL) was added from vial 3 to the ^{18}F-KF-K222 complex and the mixture was heated five times to 90°C for 10 min with 5 s mixing between heating periods. The 0.5 mL NaOH (0.5 M) was delivered from vial 4 and heated three times to 90°C for 5 min with 5 s mixing between heating periods. After cooling for 2 min and acidifying with 0.1mol/L HCl (5 mL, vial 5), the solution was loaded onto a Sep-Pak C_{18} cartridge. The cartridge was dried using nitrogen and the product was eluted with MeCN (3 mL, vial 6) into a second reaction vessel.

2.3 Synthesis of N-succinimidyl-4-^{18}F-fluoro-benzoate, ^{18}F-SFB

The 4-^{18}F-fluorobenzoic acid was eluted from the Sep-Pak C18 cartridge directy to the reaction vessel 2, and the 40 μL tetrapropylammonium hydroxide solution (1 mol/L in water) was added in the second reaction vessel previously. The mixture was heated at 116°C and evaporated to dryness. After cooling, a solution of TSTU (12 mg) in anhydrous MeCN (0.8 mL) was delivered to the reaction vessel from vial 11 and the mixture was heated three times to 90°C for 5 min with 5 s mixing between heating periods. After cooling for 2 min and acidified with 0.1mol/L HCl (5 mL, vial 12), the solution was loaded onto a Sep-Pak C_{18} cartridge. Finally, the ^{18}F-SFB was eluted with 3 mL MeCN (vial 13). The product was analyzed using radio-HPLC and radiochemical purity was evaluated.

2.4 Conjugation of ^{18}F-SFB to NGA

The MeCN solution of ^{18}F-SFB was evaporated to dryness with a stream of nitrogen. The residue was redissolved with 50 μL MeCN. The solution of NGA (1 mg, 200 μL, 0.014 μmol) in 0.1 mol/L borate buffer (pH 9.0) was added and reacted for 30 min at room temperature. The crude product was loaded onto a PD-10 column, eluted with 0.05 mol/L phosphate buffer (pH 7.5). After purification, the radiochemical purity was evaluated by radio-HPLC.

2.5 Radiochemical analysis

Analytical HPLC was performed using a Lichrospher C18 reversed-phase column (4.6×250 mm, 5 μm). The column effluent was monitored using a UV detector (Waters 2487, USA) and a flow scintillation analyzer (Radiomatic 610TR, Perkin-Elmer, USA) for radio-activity. ^{18}F-SFB was analyzed using the solution of H_2O and MeCN (v/v =55:45) with 0.1% trifluoro-acetic acid (TFA) as mobile phase at flow of 1ml/min; UV (λ=254 nm).

^{18}F-FB-NGA was analyzed with a TSK-GEL G2000SW$_{XL}$ column (7.8×300 mm) using 0.1 mol/L PB, 0.9% NaCl and 0.05% NaN_3 as mobile phase at flow of 1.0 mL/min; UV (λ=280 nm). ^{18}F-FB-NGA was incubated at room temperature for 4 h. The radiochemical purity (RCP) was evaluated by radio-HPLC at every single hour.

2.6 Biodistribution

Biodistribution of ^{18}F-FB-NGA in normal mice was studied. ^{18}F-FB-NGA (200 μL, about 0.37 MBq contained about 3 μg NGA) was injected by the tail vein. At the selected time points (10, 30 and 60 min), mice (n=5 at each time point) were sacrificed, and major organs and tissues were collected and weighed. The radioactivity in these tissues was measured using a gamma counter (1470 Automatic Gamma Counter, Perkin-Elmer, USA). The results were presented as the percentage injected dose per gram of tissue (% ID/g). For each mouse, the radioactivity of tissue samples was calibrated against a known aliquot of the injected activity. The mean uptake (% ID/g) for each group of animals was calculated with standard deviations.

2.7 MicroPET imaging

PET scans and image analysis were performed using a microPET Inveon rodent model scanner (Siemens Medical Solutions USA, Inc.). The normal and the blocking mice were tail-vein injected with about 200 μL of ^{18}F-FB-NGA (about 3.7 MBq contained about 30 μg NGA) under isoflurane anesthesia and subjected to a 30-min dynamic scan starting after injection. The images were reconstructed by 3-dimensional ordered-subsets expectation maximization (OSEM) algorithm. The blocking mouse was pre-injected with 0.2-mL NGA (3 mg) 30-min ago.

3 Results and discussion

3.1 Radiosynthesis

^{18}F-fluorination of NGA was performed using ^{18}F-SFB (Scheme 1). ^{18}F-SFB was synthesized inside the fully automatic multifunction module with a decay-corrected radiochemical yield of 42.7 ± 5.9% (n = 8) in 55–65 min. The radiochemical purity of ^{18}F- SFB was greater than 98%, as determined by analytic HPLC. Starting with ^{18}F-F$^-$, the total radiolabeling time of ^{18}F-FB-NGA took 120±10 min, including final purification. Labeled with 185–1850 MBq ^{18}F-SFB, the specific activity of ^{18}F-FB-NGA was estimated to be 7.83–78.3 TBq/mmoL. After purifying with PD-10 column, the radio chemical purity of ^{18}F-FB-NGA was above 98% as determined by radio-HPLC. ^{18}F-FB-NGA is stable for up to 4 h. The overall radiochemical yield with decay correction was 25–30%.

Yields for the conjugation correlate with several reaction parameters, such as the pH value of the reaction mixture and the initial protein concentration. As shown in Table 1, the radiochemical yield was dependent on the pH value. NGA was labeled with ^{18}F by coupling with ^{18}F-SFB under a basic condition. The percentage yield of ^{18}F-FB-NGA gave a best labeling yield by the pH= 9 at 30 min. The radiochemical yield of ^{18}F-FB-NGA increased from 4.3% to 58.1% with the concentrations of NGA from 0.1 to 5.0 mg/mL at pH=9 (Table 2). We obtained lower radiochemical yields when the concentration of NGA is less than 5 mg/mL.

Starting with ^{18}F-F$^-$, the ^{18}F-SFB was synthesized by three-step reaction. The NGA was reacted with activated ester ^{18}F-SFB through ε-amino groups of lysine residues under basic condition. The coupling yield for NGA is relatively lower than HSA. Because many ε-amino groups of lysine of NGA have been coupled with galactose groups, its coupling with ^{18}F-SFB is lower than that of HSA.

Table 1 Dependency of the radiochemical yield on the pH for radiolabeling of NGA with ^{18}F-SFB

pH	Concentration of NGA (mg/ml)	Radiochemical yield (%)
8.5	0.5	5.2
9.0	0.5	9.8
9.5	0.5	7.1
10.0	0.5	6.9
10.5	0.5	4.2

Table 2 Dependency of the radiochemical yield on the protein concentration for radiolabeling of NGA with ^{18}F-SFB

NGA (mg/mL)	pH	Radiochemical yield (%)
0.1	9.0	4.3
0.5	9.0	9.8
1.0	9.0	24.3
2.0	9.0	34.1
5.0	9.0	58.1

3.2 Radiochemical analysis

The HPLC chromatograms of ^{18}F-SFB and ^{19}F-SFB were presented in Fig.1. The resulting ^{18}F-SFB was determined with a radiochemical purity of 98.2% at the same retention time as ^{19}F-SFB. The retention time of ^{18}F-SFB in our gradient system was 10.4 min.

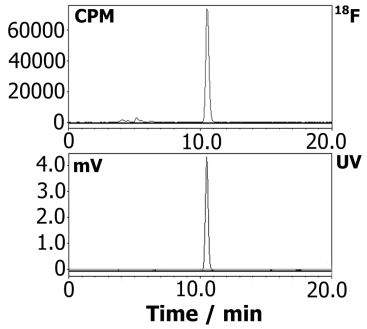

Fig.1 The chromatograms of the purified ^{18}F-SFB characterized by a radioactivity detector and ^{19}F-SFB by a UV detector (254 nm) in the same analytical HPLC condition. The resulting ^{18}F-SFB was determined with a radiochemical purity of 98.2% at the same retention time as ^{19}F-SFB.

Fig.2 shows the HPLC characterization profile of the ^{18}F-FB-NGA and NGA. The resulting ^{18}F-FB-NGA was determined with a radiochemical

purity of 98.6% at the same retention time as NGA. The retention time of ^{18}F-FB-NGA was 6.8 min.

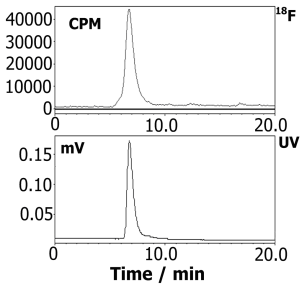

Fig.2 The chromatograms of purified ^{18}F-FB-NGA characterized using a radioactivity detector and NGA using a UV detector (280 nm) in the same HPLC condition. The resulting ^{18}F-FB-NGA was determined with a radiochemical purity of 98.6% at the same retention time as NGA.

3.3 Biodistribution

To evaluate tissue distribution characteristics of ^{18}F-FB-NGA, we performed a biodistribution experiment using ICR mice. The data expressed as the percentage administered activity (injected dose) per gram of tissue (%ID/g) (Table 3). ^{18}F-FB-NGA showed well liver accumulation. The liver uptake was 39.47 ± 3.42 at 10 min post-injection time; and 12.12 ± 6.11, at 30 min; and 5.39 ± 0.92%ID/g, at 60 mi. While the kidney uptakes were 11.19 ± 6.28 and 29.96 ± 4.27%ID/g at 10 and 30 min post-injection. The radioactivity in blood decreased rapidly. At 10 min after injection, the radioactivity concentration in blood was only 1.69 ± 0.21%ID/g. The results of biodistribution indicate that the ^{18}F-FB-NGA has high affinity with the ASGP receptor and may get a quality imaging. It makes possible to diagnose liver disease by a non-invasive method. ^{18}F-FB-NGA could be used as a receptor-specific radiopharmaceutical with potential applications in liver imaging for the evaluation of hepatocytic function.

Table 3 Biodistribution of ^{18}F-FB-NGA in ICR mice (%ID/g)

Tissues	10 min	30 min	60 min
Brain	0.16±0.02	0.13±0.02	0.09±0.01
Heart	2.86±0.66	1.85±0.30	1.26±0.16
Liver	39.47±3.42	12.12±6.11	5.39±0.92
Spleen	7.24±1.67	5.24±1.12	2.08±0.20
Lungs	5.45±0.63	5.26±1.52	3.12±0.60
Kidneys	11.19±6.28	29.96±4.27	20.33±3.48
Stomach	0.71±0.14	0.93±0.52	0.41±0.11
Small intestine	1.58±0.32	1.65±0.48	1.00±0.35
Pancreas	0.89±0.12	1.25±0.14	0.63±0.17
Muscle	0.83±0.18	0.66±0.12	0.49±0.07
Fat	1.30±0.28	1.37±0.36	0.91±0.35
Gonad	3.67±2.14	1.02±0.50	0.53±0.21
Thyroid gland	0.55±0.59	1.45±1.04	0.76±0.18
Bone	2.36±0.56	1.30±0.20	0.93±0.13
Blood	1.69±0.21	1.67±0.21	0.96±0.49

3.4 MicroPET imaging

Dynamic microPET scans were performed on the normal and block groups, and the selected coronal images at different time points after injection of ^{18}F-FB-NGA are shown in Fig.3. The normal and block groups were significantly different, especially in the heart and liver. The normal group showed low cardiac uptake and high liver uptake at 5 min after injection. The liver was clearly visible with high contrast to background, and there were no significant uptakes in other organs in the abdomen at 10 min after injection. After 30 min, the outline of liver was still clear.

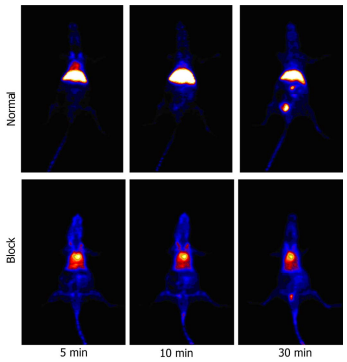

Fig.3 Coronal microPET images of mice. The upper is the normal group images at 5, 15, and 30 min after injection of ^{18}F-FB-NGA (3.7 MBq). The lower is blocking group images at 5, 15, and 30 min after injection of ^{18}F-FB-NGA (3.7 MBq) after using free NGA as blocking agent (3 mg per mouse).

On the contrary, the liver accumulation was significant lower after blocking, and the outline of liver was vague. There was no significant uptake in the liver after injection in the block group. The block group showed high cardiac uptake during the 30 min. The microPET imaging studies with the normal and the block groups clearly showed the ASGP receptor-targeting avidity and specificity of the imaging agent ^{18}F-FB-NGA *in vivo*.

The microPET of ^{18}F-FB-NGA was evaluated with high liver accumulation and certain retention. The liver uptake was decreased significantly with free NGA after blocking. The block group showed high cardiac uptake. The result of microPET coincided with biodistribution. Both of the experiments showed high affinity of ^{18}F-FB-NGA with the ASGP receptor.

4 Conclusion

The NGA was successfully labeled with ^{18}F using the prosthetic labeling group ^{18}F-SFB. Purified with PD-10, the ^{18}F-FB-NGA was got with high radiochemical purity (>98%). *In vivo* biodistribution showed that it had high liver uptake. The uptakes in other organs were low. The specific binding of this radiotracer to the ASGP receptor was also confirmed by microPET imaging study. ^{18}F-FB-NGA could be used as a hepatocyte-targeting agent to evaluate hepatic function. Furthermore, we will make the labeling more efficient, and examine the hepatic function in some hepatic injury animal models.

References

1 Kokudo N, Vera D R, Makuuchi M. Nucl Med Biol, 2003, **30:** 845–849.

2 Philippe C R, Ivan M D, Marty A L, *et al*. Bioconjug Chem, 2010, **21:** 589–596.

3 Stadalnik R C, Vera D R. Nucl Med Biol, 2001, **28:** 499–503.

4 Vera D R, Stadalnik R C, Krohn K A. J Nucl Med, 1985, **26:** 1157–1167.

5 Vera D R, Hoh C K, Stadalnik R C, *et al*. Radiopharmaceuticals for the study of liver and renal function, San Diego, 2003, 795–822.

6 Zhang R J, Liang G L, Wan W X, *et al*. Nucl Tech, 2000, **23:** 780–785 .(in Chinese)

7 Zhang R J, Wan W X, Tao Y H, *et al*. Chin J Nucl Med, 2001, **21:** 55–58.

8 Cai G M, Jiang M J, Zhou Y Y, *et al*. Pharmazie, 2011, **66:** 761–765.

9 Zhou G L, Jiang M J, Zhang R J, *et al*. Nucl Tech, 2008, **31:** 633–636 .(in Chinese)

10 Becaud J, Karramkam M, Mu L, *et al*. J Label Compd Radiopharm, 2007, **50:** S215.

11 Wuest F, Kohler L, Berndt M, *et al*. Amino Acids, 2009, **36:** 283–295.

12 Vaidyanathan G, Zalusky M R. Nat Protoc, 2006, **1:** 1655–1661.

13 Wester H J, Hamacher K, Stocklin G. Nucl Med Biol, 1996, **23:** 365–372.

14 Wuest F, Hultsch C, Bergmann R, *et al*. Appl Radiat Isot, 2003, **59:** 43–48.

15 Yang W J, Mou T T, Peng C, *et al*. Bioorg Med Chem, 2009, **17:** 7510–7516.

16 Chen Z P, Liu C Y, Li X M, et al. Nucl Sci Tech, 2012, **23:** 40-46.

17 Haka M S, Kilbourn M R, Watkins G L, *et al*. J Label Compnd Radiopharm, 1989, **27:** 823–833.

18 Johnstrom P, Harris N G, Fryer T D, *et al*. Clin Sci, 2002, **103(Suppl 48):** 4S.